ELSEVIER

Polymer 43 (2002) 1407–1416

polymer

www.elsevier.com/locate/polymer

Real time in situ X-ray diffraction studies on the melting memory effect in the crystallization of β-isotactic polypropylene

K. Cho*, D.N. Saheb, J. Choi, H. Yang

Department of Chemical Engineering/Polymer Research Institute, Division of Electrical and Computer Engineering, Pohang University of Science and Technology, Pohang 790-784, South Korea

Received 19 March 2001; received in revised form 2 October 2001; accepted 29 October 2001

Abstract

The melting memory effect during the crystallization and heating of semi-crystalline polymers was clearly demonstrated using β-isotactic polypropylene (β-iPP). Differential scanning calorimetry and real-time in situ X-ray diffraction using a synchrotron radiation source were employed to investigate the role of the newly formed α-form crystals via phase transformation from the metastable β-form during the melting process, and to elucidate the memory effect of these new α-form crystals during the crystallization process. The evolution of the memory effect in β-iPP during the crystallization and melting processes is ideally based on the existence of locally ordered α-form in the melt. We monitored the role of this local order by preparing the melt state using a range of hold temperatures and hold times. It was found that the final melt temperature and hold time greatly affect the crystallization behavior during cooling and the phase transformation behavior during heating. Lower hold temperatures and shorter hold times lead to samples rich in α-modification, whereas longer hold times generate samples rich in β-modification during crystallization. At higher hold temperatures even a short hold time is sufficient to destroy the local order in the melt, and the resulting sample exhibits more β-modification. The results are explained on the basis of the existence of local order in the amorphous melt along with external nucleating agent during the crystallization process.

Keywords: Isotactic polypropylene; Phase transformation; Memory effect

1. Introduction

Crystalline phase transformation is a characteristic feature of β-isotactic polypropylene (β-iPP), which on heating eventually transforms from the metastable β-form to the thermodynamically more stable α-form via a recrystallization process [1–13]. The phase transformation process consists of a number of intermediate stages based on rotations and transitions of the iPP chains [14]. This process depends on the molecular structure and the regularity of chains in the crystalline order. The phase transformation is a reciprocating feature of the characteristic memory effect of crystalline order during the crystallization process.

β-iPP sample is susceptible to βα-transformation during slow heating only if it is cooled below a critical cooling temperature prior to melting and it expresses the melting memory effect [15–17]. The melting memory effect during crystallization from the melt and the tendency to βα-transformation during heating can be attributed to the formation of a very small amount of α-form within the β-spherulites through a secondary crystallization process during the cooling procedure. The memory effect induces βα-transformation during the partial melting of the β-phase. The melting memory effect has been observed in studies on self-nucleation [18,19], and past work has focused on the formation of spherulites and their development. In the case of α-iPP, the memory effect is accompanied by a change in the magnitude of the birefringence of the spherulites. This change is linked to the different impacts of lamellar branching on the initial crystallization and recrystallization processes [20]. In the case of β-iPP, however, the memory effect depends on the thermal history of the sample and is accompanied by recrystallization during annealing [21].

One explanation for the melting memory effect in β-iPP is that it occurs when the melt temperature and time used to prepare the amorphous sample are insufficient to create a completely disordered state. The melting memory effect arises due to the existence of residual local order in the melt, impurities and additives, which facilitate self and/or heterogeneous crystallization of the α-form within the β-phase. The presence of these seeds for α-form order induces a recrystallization process during the partial

* Corresponding author. Tel.: +82-54-279-2270; fax: +82-54-279-8269.
E-mail address: kwcho@postech.ac.kr (K. Cho).

0032-3861/02/$ - see front matter
PII: S0032-3861(01)00729-7

melting of the β-phase, and is assisted by the structural and thermodynamic instability of the β-phase [15,16]. Under controlled heating the β-form crystals begin to melt, with βα-transformation taking place simultaneously via the recrystallization process. At this junction three phases exist: molten β-form, newly formed βα-crystallites (α') and original α-form crystals within the β-phase. Further increase of the temperature transforms the sample into a controlled melt state. The existence of locally ordered α-form at this stage, immediately after melting, is responsible for the memory effect during the crystallization process.

The melted sample contains well-dispersed β-nucleating agent, which induces heterogeneous nucleation of the α-form at lower super-cooling temperatures, and β-nucleation at higher super-cooling temperatures during crystallization. The contributions of the individual phases can be approximated by the area under the melting endotherm. In scientific terms, β-iPP (i.e. the iPP containing β-nucleating agent) is a good model system to investigate the effect of local order in the melt and the characteristic memory effect caused by self-nucleation during the crystallization and subsequent melting processes, irrespective of the presence of β-nucleating agent. This unique behavior of β-iPP provides an opportunity to investigate and understand the memory effects and consequences of crystalline transformation.

To investigate the melting memory effect in β-iPP, the present study focuses on the residual local α-form order in the melt, and the crystalline memory effect during the cooling process. This residual α-form crystalline order induces the formation of the α-form within the β-phase via self-nucleation during crystallization from the melt. This process causes the phase transformation during the melting procedure. The function of the local order and its memory effect were investigated using differential scanning calorimetry (DSC) and real-time in situ WAXD experiments. To monitor the changes in microstructure and the memory effect during crystallization, the sample was held for pre-determined durations (hold times) at different final fusion temperatures (hold temperatures) prior to characterization. The results were analyzed for the existence of local order in the amorphous melt and the role of this order in the manifestation of the memory effect during crystallization. Our results represent the first documentation of the melting memory effect of β-iPP using real-time in situ X-ray diffraction studies. This paper also takes into consideration temperature–time kinetics such as the effect of the final fusion temperature and hold time on the in situ characterization.

2. Experimental

2.1. Material

The isotactic polypropylene (iPP) used in this study was commercial molding grade Daelim Poly PP, procured from Daelim Co. Ltd., Korea. The β-nucleating agent, 'NJSTAR', was received from New Japan Co. Ltd., Japan. The materials were used as received.

2.2. Sample preparation

The iPP pellets were thoroughly pre-dried before use and then melted in a Brabender batch mixer PL-2100 model at 220 °C and 75 rpm. The β-nucleating agent (0.2 wt% of iPP) was added to the iPP melt and mixed for 3 min to obtain a homogeneous mixture. The entire experiment was carried out under nitrogen atmosphere to avoid thermo-oxidative reactions.

2.3. Differential scanning calorimetry

DSC measurements were carried out in a Perkin–Elmer DSC-7 under nitrogen atmosphere. The sample (β-iPP) was melted at a moderate rate (10 °C/min) in the first heating up to 200 °C, and was then cooled to 50 °C at the same rate. The crystallized sample was slowly reheated at 3 °C/min by maintaining a low heating profile to record the thermal transition in the compounded sample. The second heating thermogram was used to understand the phase transformation and melting memory effect of the β-iPP sample

2.4. Real time X-ray diffraction studies

Wide-angle X-ray scattering experiments were conducted using a synchrotron X-ray radiation source (3C2, 4C1 beam line, wavelength 1.598 Å) at the Pohang Accelerator Laboratory, Korea. A thin sample of β-iPP (about 1 mm thickness) was prepared in a compression molding machine at 200 °C. The sample was maintained at this temperature for 10 min and then isothermally crystallized at 100 °C for 40 min to achieve complete crystallization. This isothermally crystallized sample was used for the X-ray diffraction studies. The real-time in situ WAXD pattern was taken every 10 s during the melting and crystallization. The heating rate in these experiments was 5 °C/min and cooling was not controlled. The sample was held at a range of melt temperatures (T_h), viz. 168, 178 and 188 °C for different hold times (t_h). The WAXD pattern of the sample was also recorded during cooling under the conditions described earlier. The scattering intensity was corrected for background scattering.

2.5. Evaluation of the β-modification

The relative amount of β-modification can be estimated from the *K*-values [1] of the samples, calculated using the definition

$$K = I_{(300)\beta}/(I_{(300)\beta} + I_{(110)\alpha} + I_{(040)\alpha} + I_{(130)\alpha}) \quad (1)$$

where $I_{(110)}$, $I_{(040)}$, and $I_{(130)}$ are the intensities of the three

strong equatorial α-form peaks due to the (110), (040) and (130) planes located at $2\theta = 14.2$, 17 and 18.8°, respectively, and $I_{(300)}$ is the peak intensity due to the (300) plane in the β-form located at $2\theta = 16.2°$. The K value is zero in the absence of the β-form and unity if only the β-form is present. Fig. 1 shows typical WAXD patterns from pure samples of the β-form and α-form and from a sample comprising a mixture of these two forms of the iPP sample prepared in our laboratory.

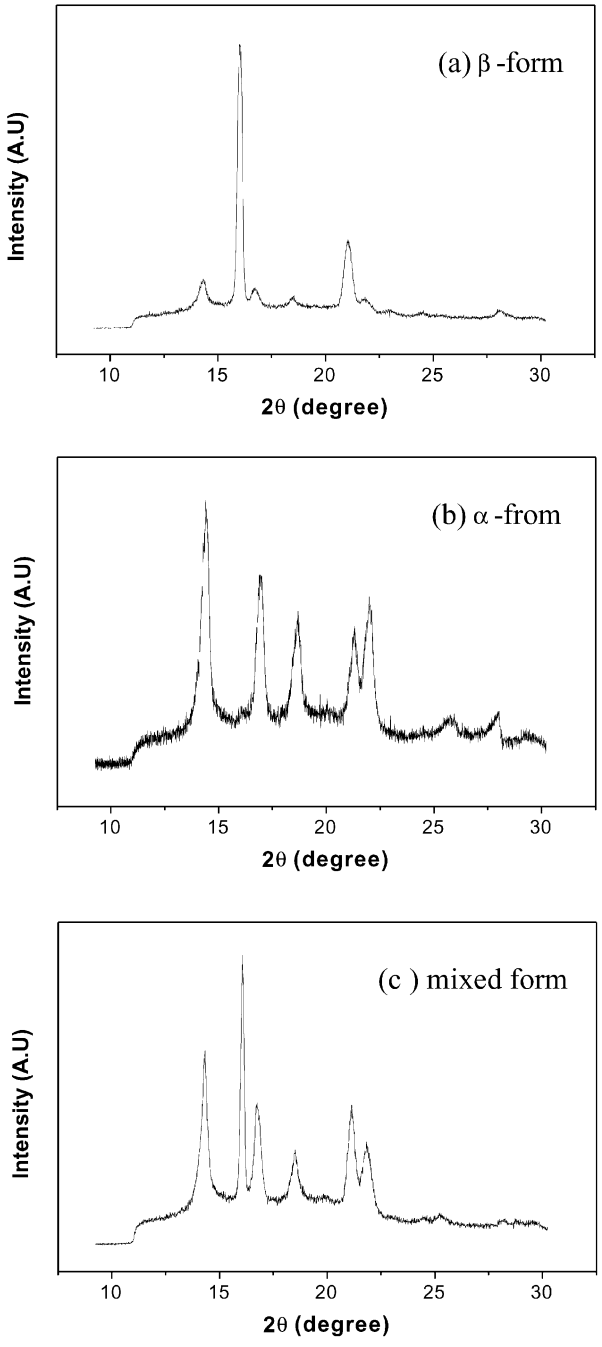

Fig. 1. Typical X-ray diffraction patterns showing the polymorphism of iPP: (a) α-form, (b) β-form and (c) mixed-form crystals (both α-form and β-form).

3. Results and discussion

3.1. Melting memory effect and phase transformation studies in β-iPP by differential scanning calorimetry

The melting and crystallization behavior of iPP was studied using various methods. A common feature among these results was the observation of clear multiple melting endotherms [21–23]. The existence of multiple endotherms has been attributed to the presence of different crystalline modifications in different degrees of perfection and size, which leads to the simultaneous melting and reorganization or recrystallization of the crystallites [24]. The difference between the α- and β-crystalline forms of iPP was further explored and attempts were made to separate the polymorphs of iPP. Special effort was dedicated to separating the α- and β-forms, of which the β-form is thermodynamically less stable and melts at lower temperatures and recrystallize as the stable α-form [25–27].

Fig. 2 shows typical DSC thermograms measured during the first heating of the original sample and the subsequent heating of the β-iPP sample prepared by the controlled cooling of the sample after the first heating. These thermograms clearly show that the melting characteristics of β-iPP are highly dependent on the thermal history of the sample. The heating thermogram of the original sample, which was prepared in a batch mixer and air-cooled to room temperature without controlling the cooling rate, exhibits two separate melting peaks at 165 and 146 °C due to melting of the α-form and β-form, respectively (Fig. 2a). An interesting feature of this thermogram is that it confirms the presence of α-phase in the prepared β-iPP. The α-form peak is due to the existence of α-form crystals within the β-phase that come from the original sample, and is found irrespective of heating rate [15,16]. It is worth noting the small endothermic peak followed by a small exothermic peak that occur at around 150 and 153 °C, respectively. A possible explanation for this behavior is that during heating ββ-recrystallization (β′) takes place within the β-modification to stabilize the β-phase, which is melting above the usual β-modification (at 150 °C). The small exothermic peak at 153 °C is due to the recrystallization of the metastable β-phase into α-phase, which can be clearly observed under slow heating (3 °C/min), shown in the second heating thermogram (Fig. 2b).

The formation of the α-phase by the β → α-recrystallization is unavoidable, even when no α-nuclei are present in the amorphous melt [27]. Because of the characteristic memory effect of the α-form, α-nuclei will crystallize within the β-phase during cooling process. The second heating thermogram (Fig. 2b) makes clear the tendency towards the melting and reorganization of β-form crystals during the heating process. This thermogram clearly shows the effect of thermal pre- and/or post-history of the sample, making evident the memory effect in the β-iPP and its susceptibility towards phase transformation. The effect occurs only if the

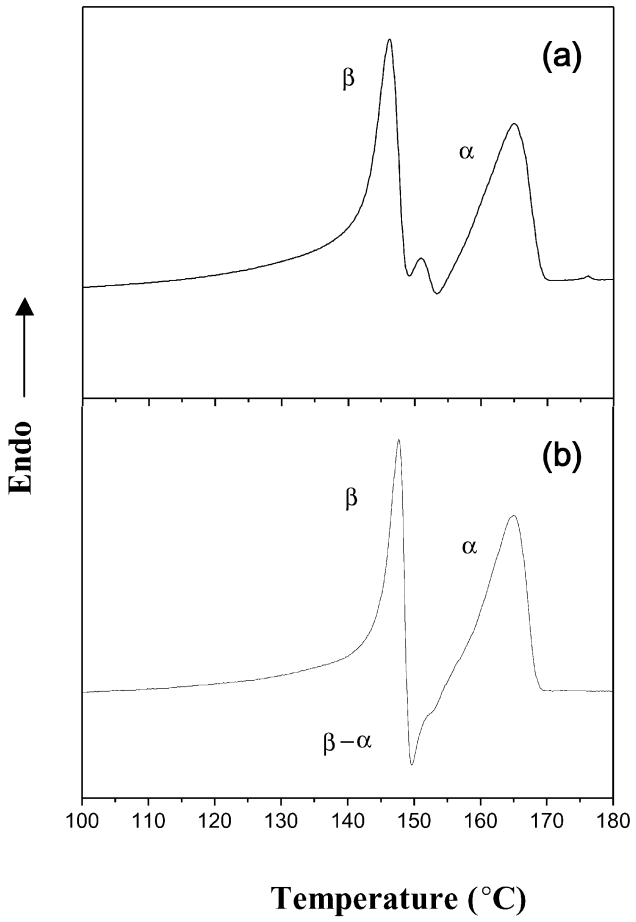

Fig. 2. Typical DSC melting thermograms of β-form iPP: (a) first heating (10 °C/min) and (b) second heating (3 °C/min).

sample was cooled below a critical cooling temperature prior to melting. Our results are in accordance with reported values [21] and confirm that βα-transformation is not a general of β-iPP, but instead is associated with a particular thermal history of the sample. The second melting thermogram was analysed to further interpret the phase transformation results.

As described earlier in the discussion of the second heating thermogram (Fig. 2b), the β-iPP sample exhibits its first melting endothermic peak at about 148 °C followed by an exothermic peak at 150 °C and second endothermic peak at around 165 °C. It is important to note that the onset of the first melting peak is at 110 °C, indicating the commencement of the melting of the metastable β-form (this is later supported by XRD studies), and reaches a maximum at 148 °C (peak temperature). The completion of melting of the β-form and start of the recrystallization of β- to α-modification (α') occur simultaneously and the peak due to recrystallization reaches a maximum at 150 °C during the melting process. The recrystallization of β- to α-form is superimposed with the onset melting of α-form crystals. The peak melting temperature of α-form is at around 165 °C, melting is complete at 168 °C. Even though the sample is heated to 200 °C, we assume that β-iPP is in the controlled amorphous melt-state at this fusion temperature. Further investigations were based on this concept.

In the second heating thermogram, the endothermic melting peak of the β-form is superpositioned with the exothermic peak of recrystallization, and the melting peak of the α-form is the summation of the melting peak due to originally existing α-crystals and the peak due to α-form newly created by recrystallization. At this junction, where the phase transformation is taking place, β-iPP is partially melted and the β-phase can be visualized as a supercooled

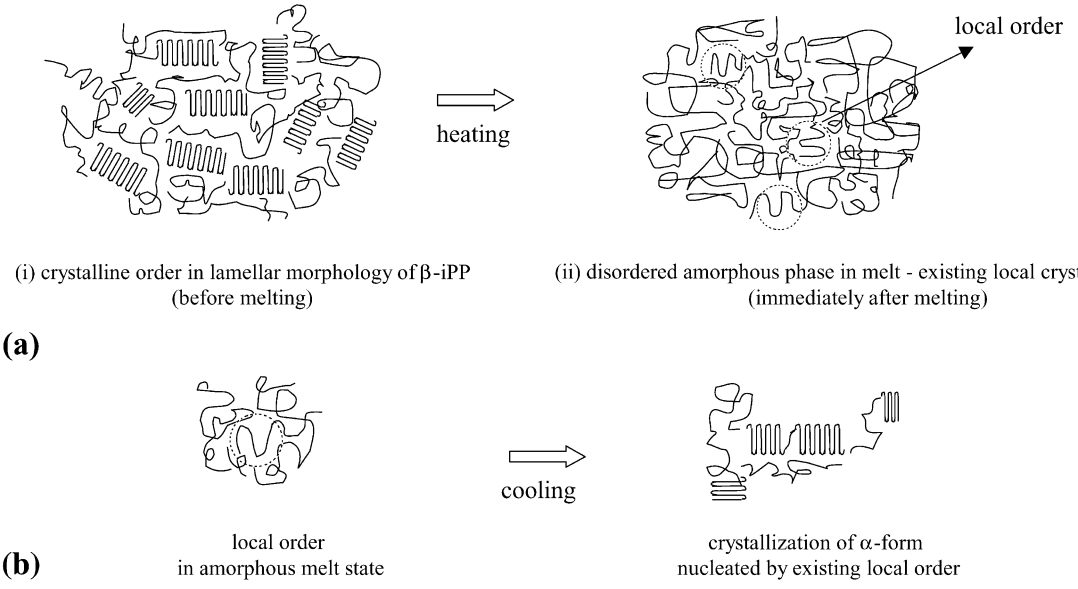

Fig. 3. (a) Schematic representation of crystalline order in β-iPP; (i) before melting, (ii) local order immediately after melting (b) α-nucleation initiated by existing local order in the melt during the cooling process.

liquid for α-form crystals, with the tendency to recrystallize into the α-form.

Fig. 3a shows schematic representations of the crystalline order in β-iPP before melting and the locally ordered α-phase structure in the melt, immediately after melting. This local order in the melt induces the recrystallization of the α-form during the cooling process, as shown in Fig. 3b. The evolution of this simultaneous melting and recrystallization behavior involves the melting memory effect of β-iPP during the melting process, and is supported by the existence of local-order of α-form in the amorphous melt.

The melting memory effect and its tendency to recrystallization is due to the formation of a very small amount of α-form crystals within the β-phase. In addition, it is responsible for βα-recrystallization during second heating, which occurs in spite of the presence of β-nucleating agent. This behavior is mainly due to the structural and thermodynamic instability of β-phase. A similar conclusion was derived from a study of the annealing and melting behavior of β-iPP [28]. The strong memory effect exhibited by recooled samples, and the existence of local order, may also be responsible for the memory effect. It is important to emphasize that the marked differences in the peak temperatures in the first and second melting thermograms are due to differences in the pre-thermal history of the sample.

3.2. Real-time X-ray diffraction studies of the phase transformation ($\beta \rightarrow \alpha$) during melting and crystallization

Fig. 1 shows characteristic WAXD patterns of (a) pure β-form, (b) pure α-form and (c) the mixed form of iPP. In this figure, the diffraction peaks of the (300) plane of the β-form and those of the (110), (040) and (130) planes of the α-form are evident [29,30]. The structural transformations in β-iPP that occur during melting and crystallization were investigated by real-time in situ WAXD studies using a synchrotron source. Fig. 4 shows the in situ WAXD pattern profiles of β-iPP (a) during melting and (b) during crystallization. WAXD pattern profiles were recorded at various melt temperatures to investigate the effect of final fusion temperature on the phase transformation.

In the melting procedure, the sample was heated at 5 °C/min and the in situ diffraction pattern profile was recorded every 10 s for each pattern. At the initial stage ($t = 0$ s) the sample exhibited a high intensity peak characteristic of the (300) plane in the β-form (Fig. 4a). Also evident at this time, however, is a very small peak characteristic of the (110) plane of the α-form, indicating the existence of α-form in the pure β-iPP sample. As the heating process progresses the β-form crystals begin to melt, causing the peak intensity of β(300) plane to diminish. Meanwhile, the α-form crystals begin to nucleate, as evidenced by the appearance of the diffraction peaks corresponding to the α(110), (040) and (130) planes as the temperature increases. It is worth considering here that the β-form crystals are

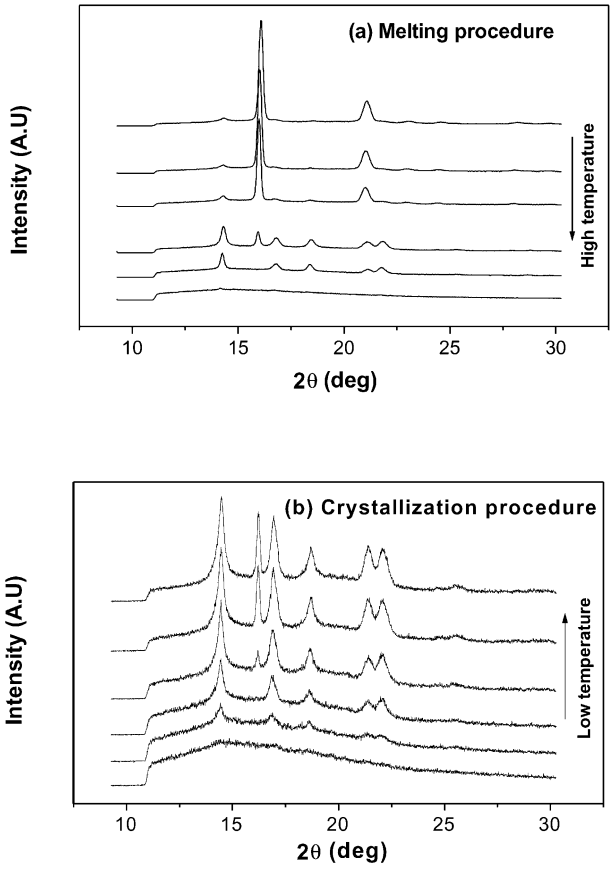

Fig. 4. In situ XRD pattern profile of β-iPP; (a) during melting and (b) during the crystallization process.

melting and then re-crystallizing into the thermodynamically stable α-form (α′) during the melting process. As heating is continued a temperature is reached where the β-form and α-form crystals coexist, and further increase of the temperature leads both crystal forms to return to an amorphous molten state at 168 °C. This temperature is comparable with that of the DSC results, in which it was denoted as the final fusion temperature (T_f) of β-iPP. As described in an earlier section, immediately after melting at this temperature there still exist some locally ordered α-form crystals, because this temperature is far below the equilibrium melting temperature. The existence of local order in the amorphous melt along with the presence of an external nucleating agent are schematically represented in Fig. 3.

The relative amount of β-form in β-iPP was determined quantitatively by calculating the *K*-value (Eq. (1)). The temperature dependence of the *K*-value during the melting procedure is shown in Fig. 5a, and confirms that a constant *K*-value ($K = 0.88$) is maintained up to 113 °C. The onset of β-form melting occurs at around 114 °C. Above this temperature, the *K*-value is found to decrease with increasing temperature. Over the temperature range 135–148 °C the *K*-value decreases sharply from 0.79 to 0.01, after which it remains almost constant. This region is the sharp

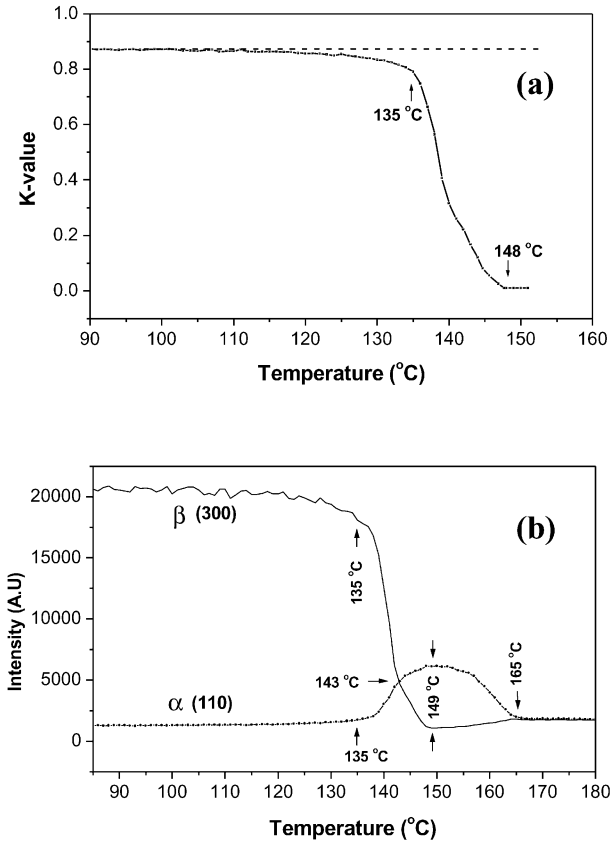

Fig. 5. (a) *K*-value as a function of temperature during the melting of β-iPP. (b) XRD peak intensities of the β(300) and α(110) plane peaks as a function of temperature during the melting procedure.

melting and recrystallization temperature zone for β-form crystals, which is supported by the DSC results (Fig. 2b). It is noteworthy that the *K*-value does not fall to zero until the final melt temperature. This may be either due to the presence of residual nuclei of β-form crystals in the polymer melt, for which there is no experimental evidence and/or limitations in the method of calculating the *K*-value.

Fig. 4b shows the in situ diffraction pattern profile during cooling from the amorphous melt state to below the crystallization temperature of the β-form. At around 168 °C, the conditions were held constant for $t_h = 60$ s in order to obtain a uniform melt, after which the sample was crystallized by decreasing the temperature. At higher temperatures (lower super coolings), α-form crystals begin crystallizing first. This crystallization might be initiated by athermal nucleation by the β-nucleating agent or self-nucleating by the local order. On further decrease of the temperature, β-form crystals, nucleated by external β-nucleating agent, begin crystallizing. Both crystalline phases crystallize simultaneously during further lowering of the temperature, leading to mixed-type crystals. We assumed that all of the crystals would be melted after holding the sample at 168 °C for 60 s, leaving only the β-nucleating agent in the melt, and that β-form crystals would be the first to crystallize. However, upon cooling from the melt α-form crystals appear first, which is a quite unexpected result. This result confirms that the molten α-form crystals exhibit a characteristic memory effect during the crystallization process from the melt, which is referred to as the melting memory effect.

The peak intensities of the β-form (300) plane and the α-form (110) plane are plotted against the temperature during the melting process in Fig. 5b. The β-form peak intensity begins to decrease at around 130 °C, followed by a sharp decrease in the region 135–149 °C. The variation of the peak intensity for the α(110) plane is interesting. The onset of the increase in the α(110) plane peak intensity occurs at around 135 °C, the same temperature as the onset of the sharp decrease in β(300) plane peak intensity. Further increase in α(110) peak intensity is due to the transformation of β-form into α-form. The α(110) plane peak intensity reaches a maximum at the temperature at which the β(300) plane peak intensity shows a minimum. The first intersection point of these two peaks, which occurs at approximately 143 °C, can be termed the critical equilibrium transition temperature of the two phases. This represents clear evidence of a crystalline phase transformation during the melting of β-iPP. The intensity of the α(110) plane peak reaches a maximum at 149 °C then decreases with increasing temperature until it meets the β(300) plane peak intensity at 165 °C. The temperature is the same as the peak temperature of the α-form in the DSC study, which indicated that equilibrium was achieved in the melt.

Fig. 6 shows the variation in the peak intensities of the two crystalline modifications during the crystallization process for the sample held for 60 s at the higher final fusion temperature of 188 °C. It is noteworthy that the crystallization of the β-form begins at 120 °C and is complete by 107 °C, as evidenced by the sharp increase in intensity of the β(300) plane peak. No characteristic α(110) plane peak was observed during cooling down to 90 °C, after which change in intensity was not observed. Based on these results, we extended our study to investigate the effect of

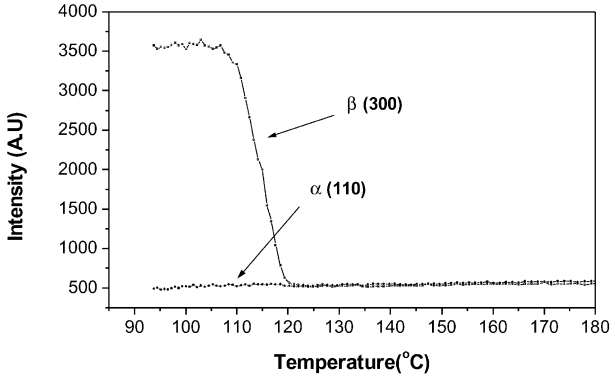

Fig. 6. XRD peak intensities of the β(300) and α(110) plane peaks as a function of temperature during the crystallization procedure from the sample prepared at $T_h = 188$ °C, $t_h = 60$ s.

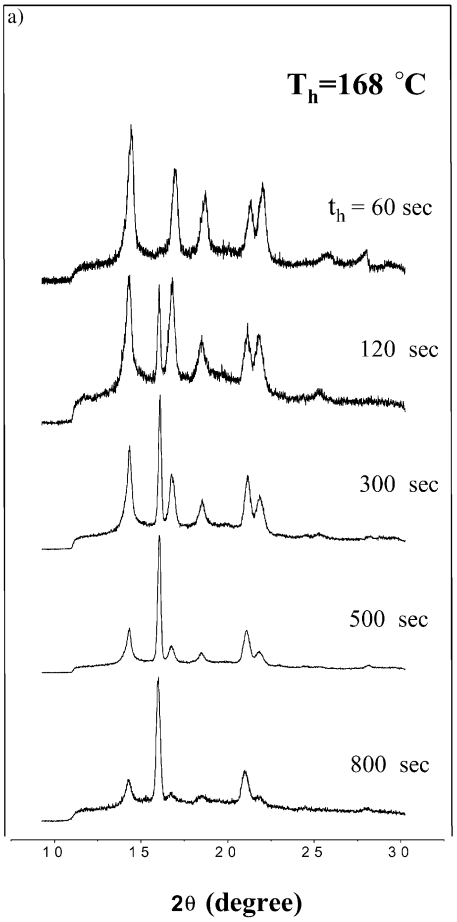

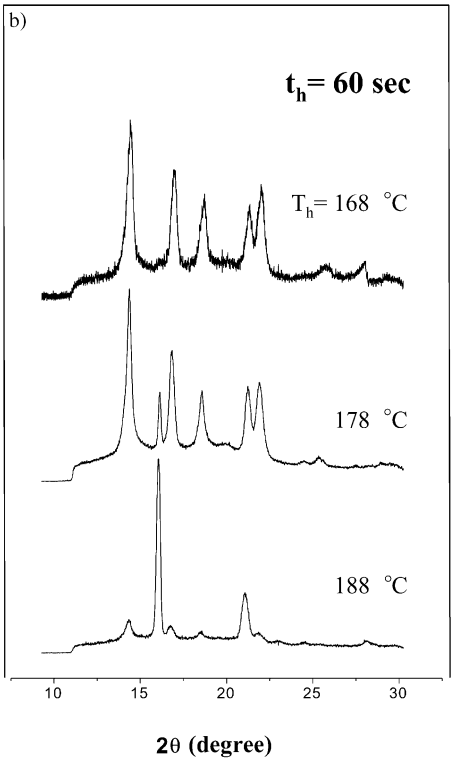

Fig. 7. XRD pattern of final crystallized β-iPP sample; (a) hold temperature T_h = 168 °C with hold times t_h = 60, 120, 300, 500 and 800 s. (b) hold time t_h = 60 s with hold temperatures T_h = 168, 178 and 188 °C.

the final fusion temperature on the crystalline morphology of β-iPP, considering the effects of both hold temperature and hold time.

3.2.1. Effect of hold temperature (T_h) and hold time (t_h)

The β-iPP was heated to a pre-determined final fusion temperature and the sample was held at that hold temperature (T_h) for a specific hold time (t_h). Three different hold temperatures were used, 168, 178 and 188 °C, and the hold times at these temperatures ranged from 60 to 800 s. Fig. 7a shows the X-ray diffraction patterns for the completely crystallized β-iPP samples held at 168 °C for hold times of 60, 120, 300, 500 and 800 s.

Based on the DSC and WAXD results, we used this temperature (T_h = 168 °C) to investigate the influence of hold temperature and time on the final crystalline morphology of β-iPP. At this fusion temperature, morphological reorganization may take place even in the amorphous melt, since some locally ordered α-form crystallites are present along with the β-nucleating agent. At the hold temperature of T_h = 168 °C the sample was held for t_h = 60 s and then crystallized by lowering the temperature. The WAXD pattern recorded for the completely crystallized sample is shown in Fig. 7a (Pattern 1). This pattern shows that the sample has completely crystallized into the α-form, and no characteristic peak of the β-form. For the longer hold time of 120 s, the sample contains both types of crystalline modifications, which are equally dominant. Interestingly, on further increase of the hold time to 300 s the β-form dominates the α-form. Further prolongation of the hold time to 500 and 800 s at 168 °C leads to almost complete crystallization into the β-form, with the formation of only a small fraction of α-form.

This phenomenon can be explained on the basis of a nucleation and growth mechanism [31,32]. In the melt, the polymer exists in an amorphous state that contains some minute crystalline order/local order of α-crystals. During the crystallization process, this local order initiates α-nucleation at higher temperatures, and dominates the effect of the β-nucleating agent. Increasing the hold time at the final fusion temperature causes the locally ordered α-crystals to melt; therefore, the self-nucleating capacity of the α-form slowly reduces with increasing hold time. For the sample held at T_h = 168 °C for t_h = 60 s, the crystallized sample exhibits full α-form, and local order tends to nucleate the α-modification and suppress β-nucleating activity. If the sample is held for longer times, say t_h = 120 s, there is an increase in the disturbance of the local order and a corresponding decrease in its nucleating efficiency,

and the β-nucleating agent has an activating effect (Pattern 2). Further increase of the hold time to 300 and 500 s causes an increase in the randomness of the local order, which removes the external forces hindering the β-nucleating agent and the sample shows more β-modification (Patterns 3 and 4). At the highest hold time, $t_h = 800$ s, no local order exists in the melt, which contains evenly distributed solid β-nucleating agent. After this hold time, the presence of the β-nucleating agent efficiently induces formation of β-form from the melt, as shown in Pattern 5. However, the formation of a small fraction of α-content within the β-phase is still possible, and a peak characteristic of the α-form of very low intensity is observed.

Based on the results at 168 °C, more experiments were conducted at different fusion temperatures to test the effects of hold temperature and hold time, and which of these plays a more important role in determining the crystalline modification of iPP. Three hold temperatures (T_h) were monitored, 168, 178 and 188 °C, at a range of hold times. Fig. 7b shows the WAXD pattern profiles of β-iPP for the three hold temperatures at the hold time of $t_h = 60$ s. These profiles clearly show the effect of the local order in the melt, which causes the preferential nucleation of the α-crystalline modification over the β-modification in iPP.

Immediately after the melting of the α-form at $T_h = 168$ °C, the lowest temperature considered, local order is more probable, more stable and sustained for a longer time than at the higher hold temperatures. This local order rapidly initiates α-nucleation over the β-nucleating agent (Pattern 1). Increasing the hold time at this temperature may destroy the local order, as explained earlier. Increasing the hold temperature reduces the efficiency of the local order even at the smallest hold time, and improves the efficiency of the β-nucleating agent. At $T_h = 178$ °C both types of crystalline modification are found in equal predominance, because the lowering of the local order enhances the activity of the β-nucleating agent in the initiation of β-form (Pattern 2). At the highest fusion temperature, $T_h = 188$ °C, complete β-modification is observed (Pattern 3). This arises because of the complete destruction of the local order of α-form, and the proficient role of the β-nucleating agent in the nucleation process, results in pure β-form crystals. It is worth noting that the WAXD pattern obtained from the final crystallized iPP sample at $T_h = 188$ °C, $t_h = 60$ s, resembles the pattern at $T_h = 168$ °C, $t_h = 800$ s.

Afore-mentioned results are straightforward, yet interesting, explanation for the melting memory effect of local order, and its effect on the crystalline modification in β-iPP during the crystallization process. Fig. 3 shows schematic representations of the crystalline order in β-iPP before melting and the locally ordered α-phase in the melt immediately after melting. At lower fusion temperatures and shorter hold times, the memory effect of these regions of unmelted local order has a greater influence on the crystal modification. If the hold time is increased from the low fusion temperature of $T_h = 168$ °C to $T_h = 178$ or 188 °C, the memory effect of the crystalline order is reduced. In addition, the local order exhibits less efficiency when longer hold times or higher hold temperatures are adopted before the start of the crystallization process. The phenomenon described above is based on the melting characteristics of the local order, whereas its efficiency depends on the size and number of regions of local order after completion of the melting process.

3.2.2. Dependence of the K-value on hold temperature (T_h) and hold time (t_h)

The relative amount of the crystal in β-form can be

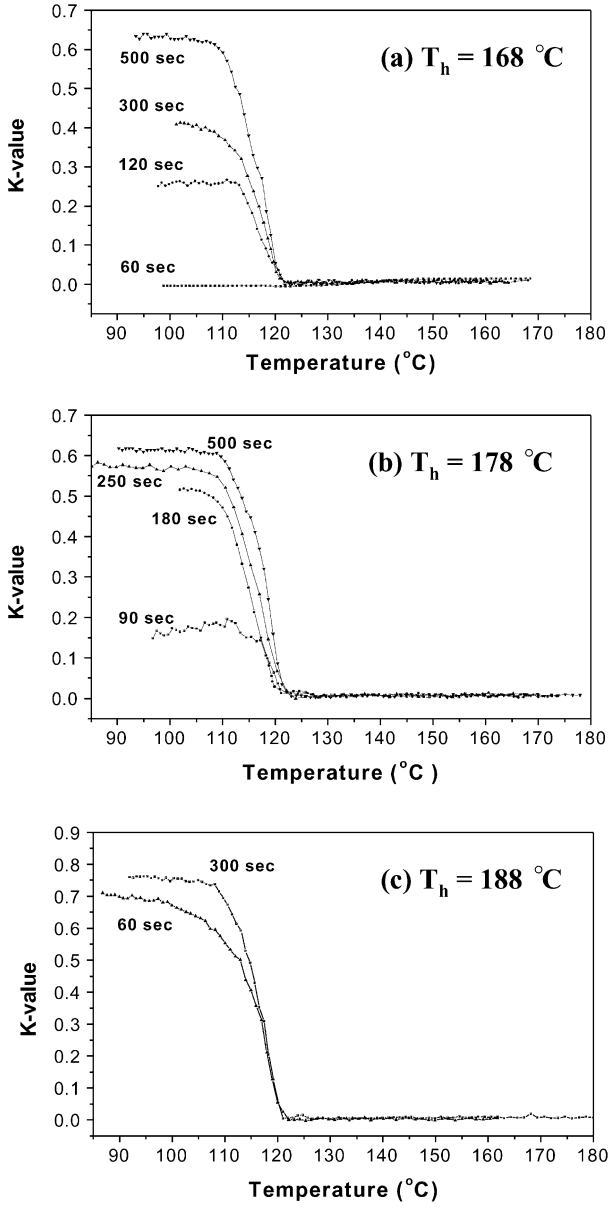

Fig. 8. *K*-value as a function of temperature during crystallization from samples prepared at hold temperatures (a) $T_h = 168$ °C, (b) $T_h = 178$ °C and (c) $T_h = 188$ °C for different hold times (t_h).

expressed by the K-value (Eq. (1)). Fig. 8 shows the temperature dependence of the K-value during crystallization at various hold temperatures and hold times. The extent of β-modification was found to increase with increasing hold time at all hold temperatures. At a hold temperature of $T_h = 168$ °C no β-modification was observed for systems held for $t_h = 60$ s, leading to a K-value of almost zero, even down to 100 °C (Fig. 8a). It is worth noting that the onset of β-modification occurs at around 121–123 °C for all hold times ($t_h = 120$, 300 and 500 s). For example, for the hold time $t_h = 60$ s, $K = 0$; for $t_h = 120$ s, $K = 0.26$; for $t_h = 300$ s, $K = 0.42$ and for $t_h = 500$ s, $K = 0.64$. Under non-isothermal crystallization conditions, the maximum extent of β-modification takes place in the temperature range 121–107 °C, and it remains constant.

Fig. 8b and (c) shows the variation in K-value for the other two hold temperatures at a range of hold times. The K-value is observed to vary significantly depending on the hold time and hold temperature. The nucleation and growth mechanism are very sensitive to final fusion temperature and hold time, discussed in an earlier section, causes the relative change in crystalline modification to vary with the conditions adopted for the investigation. The relative change in K-value for a hold time of 500 s is around 0.64 for hold temperatures of 168 and 178 °C, whereas the final K-value is very high (in the order of 0.71) for $t_h = 60$ s at $T_h = 188$ °C. This represents clear evidence for the role of local order and the effect of hold time and temperature on β-modification. The results confirm that at higher fusion temperatures even a small amount of time is sufficient to achieve complete β-modification, whereas at lower hold temperatures more time is required to destroy the local order and to overcome its memory effect. In every case, the onset of β-modification occurs in the same temperature range (121–123 °C) and its rate depends on the conditions adopted for the experimental study.

3.2.3. Dependence of diffraction peak intensities of β- and α-form on hold temperature (T_h) and hold time (t_h)

The behavior of this system was studied further by plotting the variation in the characteristic peak intensities of the β-form and α-form for the different values of T_h and t_h. Fig. 9 shows a typical example of these results, taken at $T_h = 168$ °C and $t_h = 60$, 300 and 500 s. These plots clearly show that the intensities of the characteristic β(300) and α(110) plane peaks vary in opposite manner. At every hold temperature the β(300) plane peak intensity increases with increasing hold time, whereas the α(110) plane peak intensity decreases. The onset temperature for the increase in intensity of the β(300) plane peak is in the narrow temperature region 118–121 °C (Fig. 9a), whereas the onset temperature of the decrease in intensity of the α(110) plane peak varies remarkably with hold time and temperature.

The variation in peak intensity corresponding to the β-modification shows a similar trend to the variation in

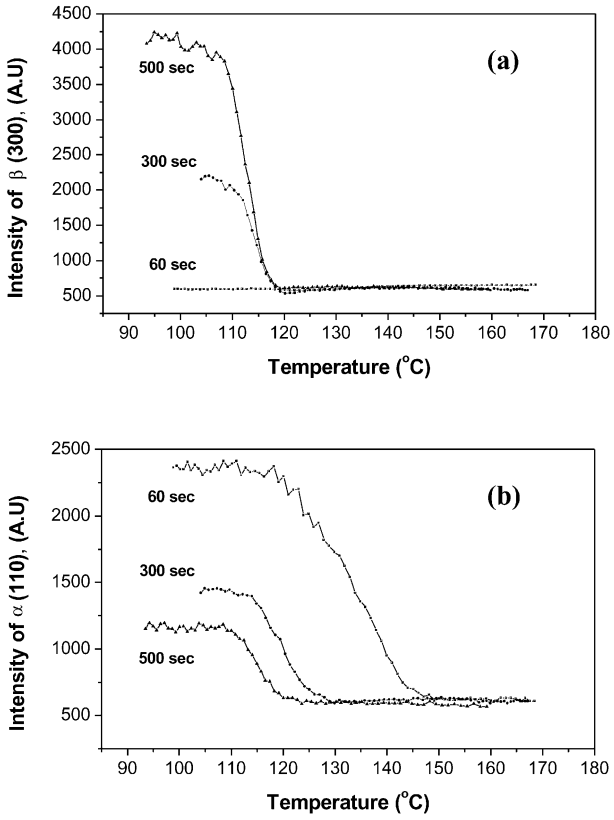

Fig. 9. XRD peak intensities of the β(300) plane and α(110) plane peaks as a function of temperature for samples prepared at a hold temperature of $T_h = 168$ °C and a range of hold times (t_h); (a) β-form and (b) α-form.

K-values, because these quantities are inter-related as per Eq. (1). The effect of local order and its nucleating efficiency at various temperatures and times is especially evident in the trends in α-modification with respect to T_h and t_h. The onset of α-modification for $T_h = 168$ °C occurs at around 148 °C for $t_h = 60$ s, whereas the onset temperatures for $t_h = 300$ and 500 s are 128 and 124 °C, respectively (Fig. 9b). As the hold time or hold temperature is increased, the onset temperature for α-nucleation decreases and is delayed because of a decrease in both local order and α-nucleation efficiency. These factors lead to an increase in β-nucleation efficiency and a consequent increase in β-modification. To further characterize this system, we plotted the crystallization initiation temperature with respect to hold time for the β(300) and α(110) plane peaks for samples at a range of hold times and temperatures. The results are shown in Fig. 10.

DSC thermograms were recorded for the crystallization of β-iPP from the melt for the samples held at $T_h = 168$ °C over a range of hold times (t_h). No significant change was observed in the cooling thermogram, which may be due to a limitation of this technique. The onset of crystallization temperature decreased with increasing hold time, and a small decrease in the crystallization peak temperature was observed. This might be due to the prolonged thermal

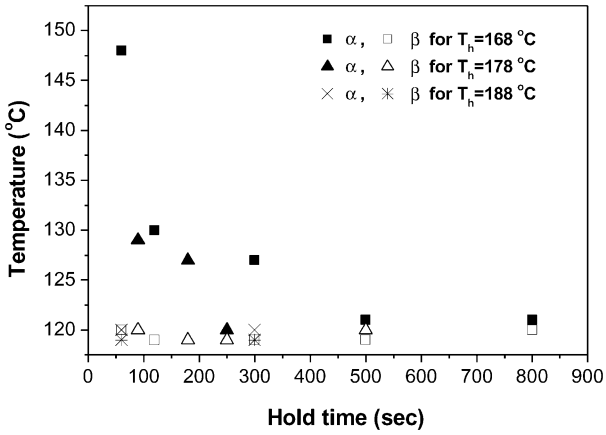

Fig. 10. Variation in crystallization initiation temperature in β-iPP at different hold temperatures and hold times.

treatment of the sample at high fusion temperature, as well as kinetic and morphological features.

4. Conclusions

β-iPP is a good model system for investigating the effect of local order in the melt, and the characteristic memory effect caused by self-nucleation, during the crystallization and melting processes, irrespective of the presence of β-nucleating agent. This unusual behavior of β-iPP provides an opportunity to investigate and to understand memory effects and their consequences for crystalline transformation.

In the present study, we investigated the melting memory effect of β-iPP in the crystallization behavior and crystalline phase transformation from metastable β-form to stable α-form using DSC and in situ WAXD studies. During the heating process, the β-form first melts and then reorganizes into the stable α-form via a phase transformation. A marked melting memory effect was also clearly observed during the crystallization process. This observation can be explained by the existence of locally ordered α-form in the amorphous melt immediately after melting. The final fusion temperature and hold time significantly affect the crystallization behavior during cooling, and the phase transformation during heating. A lower melt temperature and shorter hold time result in more α-modification because the presence of local α-form order dominates nucleation involving the β-nucleating agent. Increasing the hold time and hold temperature reverses this behavior and results in β-modification. At higher hold temperatures even a small hold time is sufficient to destroy the local order and the sample is rich in β-modification. The results suggest that a lower melt temperature and longer hold time, or a higher melt temperature and shorter hold time, are the preferred means of obtaining a high percentage of the pure and more stable β-form in iPP.

In conclusion, we have clearly demonstrated the memory effect in the semi-crystalline polymer β-iPP during the heating and crystallization process using in situ wide-angle X-ray diffraction technique and DSC.

Acknowledgements

The authors would like to thank the Ministry of Education of Korea for its financial support through its BK21 Program, the National Research Laboratory Project (Ministry of Science and Technology of Korea), and the Pohang Accelerator Laboratory for providing the synchrotron radiation source at the 3C2, 4C1 beam lines used for this study.

References

[1] Turner Jones A, Aizlewood JM, Beckett DR. Makromol Chem 1964;75:134.
[2] Addink EJ, Bientema J. Polymer 1961;2:185.
[3] Padden Jr FJ, Keith HD. J Appl Phys 1959;30:1479.
[4] Fujiwara Y. Colloid Polym Sci 1975;253:273.
[5] Fujiwara Y. Colloid Polym Sci 1987;265:1027.
[6] Lovinger AJ, Chua JO, Gryte CC. J Polym Sci, Polym Phys Ed 1977;15:641.
[7] Karger-Kocsis J. Polym Bull 1996;36:119.
[8] Karger-Kocsis J. Polym Engng Sci 1996;36:306.
[9] Karger-Kocsis J. In: Karger-Kocsis J, editor. Polypropylene: structure and morphology. London: Chapman & Hall, 1995.
[10] Jacoby P, Bersted BH, Kissel WJ, Smith CE. J Polym Sci, Polym Phys Ed 1986;24:461.
[11] Varga J. J Polym Engng 1991;1:231.
[12] Lotz B, Wittmann JC, Lovinger AJ. Polymer 1996;37:4979.
[13] New Japan Chemical Co Ltd. EP 93101000.3; JP 34088/92, JP 135892/92, JP 283689/92, JP 324807/92m (1992).
[14] Garbarczyk J. Makromol Chem 1985;186:145.
[15] Varga JJ. Therm Anal 1986;31:165.
[16] Varga JJ. Therm Anal 1989;35:1891.
[17] Varga J, Garzo G, Ille A. Angew Makromol Chem 1986;142:171.
[18] Vidotto G, Levy D, Kovacs AJ, Kolloid Z. U.Z. Polymer 1969;230:289.
[19] Chivers RA, Barham PJ, Martinez-Salazar J, Keller A. J Poly Sci, Polym Phys Ed 1982;20:1717.
[20] Lotz B, Wittmann JC. J Poly Sci, Polym Phys Ed 1986;24:1541.
[21] Varga J, Toth F. Makromol Chem Macromol Symp 1986;5:213.
[22] Cho K, Li F, Choi JS. Polymer 1998;40:1719.
[23] Guerra G, Petraccone V, Corradini P, De-rosa C, Napolitano R, Pirozzi B, Giunchi G. J Polym Sci, Polym Phys 1984;22:1029.
[24] Nabi Saheb D, Jog JP. J Polym Sci, Polym Phys 1999;37:2439.
[25] Garbarczyk J, Paukszta D. Colloid Polym Sci 1985;263:985.
[26] Elsner G, Riekel Ch, Zachmann G. Adv Polym Sci 1985;67:1.
[27] Nabi Saheb D, Kilwon Cho. Unpublished results.
[28] Zannetti R, Celotti G, Finchera A, Francescons R. Makromol Chem 1969;128:137.
[29] Shi G, Huang B, Cao Y, He Z, Han Z. Makromol Chem 1986;187:643.
[30] Forgacs P, Tolochko BP, Sheromov MA. Polym Bull 1981;6:127.
[31] Fillon B, Wittmann JC, Lotz B, Thierry A. J Polym Sci, Polym Phys 1993;31:1383 see also p. 1407.
[32] Supaphol P, Spruiell JE. J Appl Polym Sci 2000;75:337.